Borrell Tomás, MA.; Salvador Moya, MD. (2013). Sliding wear behavior of WC-Co-Cr3C2-VC composites fabricated by conventional and non-conventional techniques. Wear. 307:60-67. doi:10.1016/j.wear.2013.08.00.

Sliding wear behavior of WC-Co-Cr_3C_2-VC composites fabricated by conventional and non-conventional techniques

L. Espinosa-Fernández[1], A. Borrell[1]*, M. D. Salvador[1], C. F. Gutierrez-Gonzalez[2]

[1]Instituto de Tecnología de Materiales (ITM), Universitat Politècnica de València, Camino de Vera s/n, 46022 Valencia, (Spain)

[2]Centro de Investigación en Nanomateriales y Nanotecnología (CINN) [CSIC-UO-PA], Parque Tecnológico de Asturias, 33428 Llanera (Asturias), Spain

*Corresponding author. Address: Instituto de Tecnología de Materiales (ITM), Universidad Politécnica de Valencia (UPV), Camino de Vera s/n, 46022 Valencia, Spain. Tel.: +34 963 877 007; Fax: +34 963 877 629.

E-mail address: aborrell@upvnet.upv.es (A. Borrell)

Abstract

The present work aims are to study the dry sliding wear behavior of WC-12 wt.%Co materials, with or without addition of Cr_3C_2/VC grain growth inhibitors, and to sinter them by two different consolidation techniques: conventional sintering and spark plasma sintering (SPS). The dry sliding wear tests were performed on a tribometer with a ball-on-disc configuration using a WC-Co ball as a counterpart material with a normal contact load of 60 N, a sliding distance of 10000 m and a sliding speed of 0.1 m/s. The influence of the grain growth inhibitors and the consolidation techniques in sintered samples were related to the friction coefficient, wear rates and wear pattern damage. Samples sintered by non-conventional technique (SPS) show the best wear resistance and lower friction coefficient. The addition of inhibitors reduces the wear

rates in materials consolidated by both techniques. The differences in the wear damage are related to microstructural parameters, mechanical properties and wear rates.

Keywords: Sliding wear; Hardness; Cermets; Cutting tools

1. Introduction

WC-Co cemented carbides, where Co is a binder phase, have long been used as cutting tools [1,2], rock drill tips [3], dies [4] and wear resistant parts. This is due to the combination of mechanical properties (toughness and hardness) and excellent wear resistance behavior. In recent years, the ultrafine and nanometric WC-Co cemented carbides have received increasing attentions because of the special demands on the excellent performance of materials in the electronic and automotive industries [5].

Manufacturing WC-Co cemented carbides with fine grain sizes, in the nanometre scale, is a good method to improve their wear properties [6]. The wear resistance of WC-Co materials is related to their chemical composition and microstructure. This property generally increases with the reduction of cobalt content and with the reduction of the WC grain size [7,8]. In order to obtain the ultrafine- and nanostructure WC-Co bulk materials, several sintering methods such as conventional liquid phase sintering [9,10], hot isostatic pressing (HIP) [11], and non-conventional processes; microwave sintering [12] and spark plasma sintering (SPS) [13-18], have been developed. In particular, the SPS technique has attracted considerable attention due to a rapid heating and high applied pressures, which allows sintering

samples in a shorter time and refines microstructures in comparison with others sintering processes [7,13-18].

One of the keys to control the grain growth in ultrafine WC-Co composites is the suitable selection of the additives as WC grain growth inhibitors [17-19]. On the one hand, Sun et al. [17] evaluated the effect of different amounts of ceria nano-particles in WC-Co composites by SPS. They demonstrated that the trace nano-ceria addition effectively suppressed the abnormal grain growth of WC, leading to the uniform and fine microstructures. On the other hand, Bonache et al. [18] studied that the vanadium carbide (VC) and chromium carbide (Cr_3C_2) are effective grain growth inhibitors due to their high solubility and mobility in cobalt phase at low temperatures.

The wear behavior of cemented carbides sintered by different consolidation processes has been evaluated in dissimilar laboratory conditions and tribosystem configurations. However, the literature reports a few studies in which ultrafine or nanosized WC-Co bulk materials obtained by SPS are evaluated in dry sliding wear regarding to other consolidated techniques [16]. Picas et al. examined the efficiency of three different consolidations processes in terms of the tribological behavior. They found that the SPS bulk samples showed similar tribological properties to HVOF (High velocity oxy-fuel spray forming) coating samples, and these have better wear resistance than LENS (laser engineered net shaping) coating samples under the same sliding conditions. They concluded that the good performance of SPS bulk samples is attributed to its homogenous microstructure and greater micro-hardness values. Therefore, it is interesting to investigate the tribological behavior of nanostructured WC-Co obtained by the SPS technique in comparison with other consolidation processes.

In this work, the tribological response of WC-12 wt.%Co cemented carbides obtained by a nanopowder mixture with the addition of Cr_3C_2 and VC, and sintered by two different techniques; conventional sintering and spark plasma sintering have been studied. The influence of the grain growth inhibitors and both consolidation techniques were investigated and compared. The differences in the friction coefficient and sliding wear behavior are related to microstructural parameters and mechanical properties.

2. Experimental procedure

2.1. Materials and sintering conditions

In this work, a WC-12 wt.%Co nanometric mixture with a WC grain size of 40-80 nm, manufactured by Inframat Advanced Materials, was used as raw material. The amounts of 1 wt.%Cr_3C_2, 1 wt.%VC, and a mixture of 0.5 wt.%VC+0.5 wt.%Cr_3C_2 were added to the raw powder, which were used as WC grain growth inhibitors. Designation and compositions of the final powder mixtures are shown in Table 1.

Table 1. Designation and composition of powder mixtures.

Sintering technique	Designation	Starting mixture	Additives (wt.%)	
			Cr_3C_2	VC
Conventional sintering	N	WC-12wt.% Co	0	0
	NCr	WC-12wt.% Co	1	0
	NCrV	WC-12wt.% Co	0.5	0.5
	NV	WC-12wt.% Co	0	1
Spark plasma sintering	N-SPS	WC-12wt.% Co	0	0
	NCr-SPS	WC-12wt.% Co	1	0

	NCrV-SPS	WC-12wt.% Co	0.5	0.5
	NV-SPS	WC-12wt.% Co	0	1

The particle size of these inhibitors carbides was around 0.5-1.0 μm. The milling conditions, processing and sinterability parameters have been reported elsewhere [18,20].

Two different methods were used to sinter these mixtures: conventional sintering (CS) and spark plasma sintering (SPS).

Conventional sintering conditions: Green compacts were prepared by uniaxial pressing at 200 MPa into a steel matrix with an inner diameter of 15 mm. The samples were consolidated at 1400 ºC for 30 min under vacuum with a heating rate of 10 ºC/min (Carbolite furnace).

Spark plasma sintering conditions: The powder samples were placed into a graphite die with an inner diameter of 20 mm and cold uniaxially pressed at 30 MPa. The samples were subsequently introduced in a spark plasma sintering apparatus HP D 25/1 (FCT Systeme, Germany) and sintered at 1100 ºC for 5 min under vacuum with an applied pressure of 80 MPa and a heating rate of 100 ºC/min.

2.2. Characterization

The consolidated materials densities (relative density) were measured following the Archimedes' method with ethanol immersion, according to ISO 3369 standard [21]. The microstructures of the sintered materials were observed on the polished cross-sectioned surfaces by field emission scanning electron microscopy (FESEM, Hitachi S4100, SCSIE of the University of Valencia). The WC grain size was determined with the lineal intercept method according to standard ASTM E112 [22]. Vickers hardness

measurements were carried out by applying a load of 30 Kgf according to standard ASTM E92-72 [23].

2.3. Sliding wear test

Wear tests were carried out under dry sliding conditions using a tribometer pin-on-disc (ball-on-disc configuration) manufactured by MICROTEST MT2/60/SCM/T, according to ASTM wear testing standard G99-03 [24]. A ball of WC-6 wt.%Co cemented carbide produced by FRITSCH (Germany) with a hardness of 1480 HV_{30} and 5 mm radius was used as countermaterial. The tests were performed with the following parameters: contact load of 60 N, sliding speed of 0.1 m/s, a sliding distance of 10000 m, and a wear track radius of 3 mm. All tests were conducted in controlled conditions (23 ± 2 ºC of temperature and 60 ± 2% of relative humidity). In order to obtain a representative value of each response parameters, a series of three tests were carried out for each material. Wear tracks were analyzed by FESEM and energy-dispersive X-ray analysis (EDX).

Sample surface was polished down to 1 μm and cleaned before the wear test. The wear mass loss was obtained by weighing the samples before and after the test. Wear volume loss, V_{wear}, was determined from the measured mass loss of the samples divided by the density of each one. The wear rate, K_V, was calculated according to the Lancaster´s equation [25]:

$$k_v = \frac{V_{wear}}{F_N \times S}$$

Where, V_{wear} is the mass lost, F_N is the contact load in N and, S is the sliding distance in m.

3. Results and discussion

3.1. Microstructural and mechanical characterization

The microstructure of the cross-section of four representative consolidated materials by conventional sintering (CS) and spark plasma sintering (SPS) can be observed in Fig. 1.

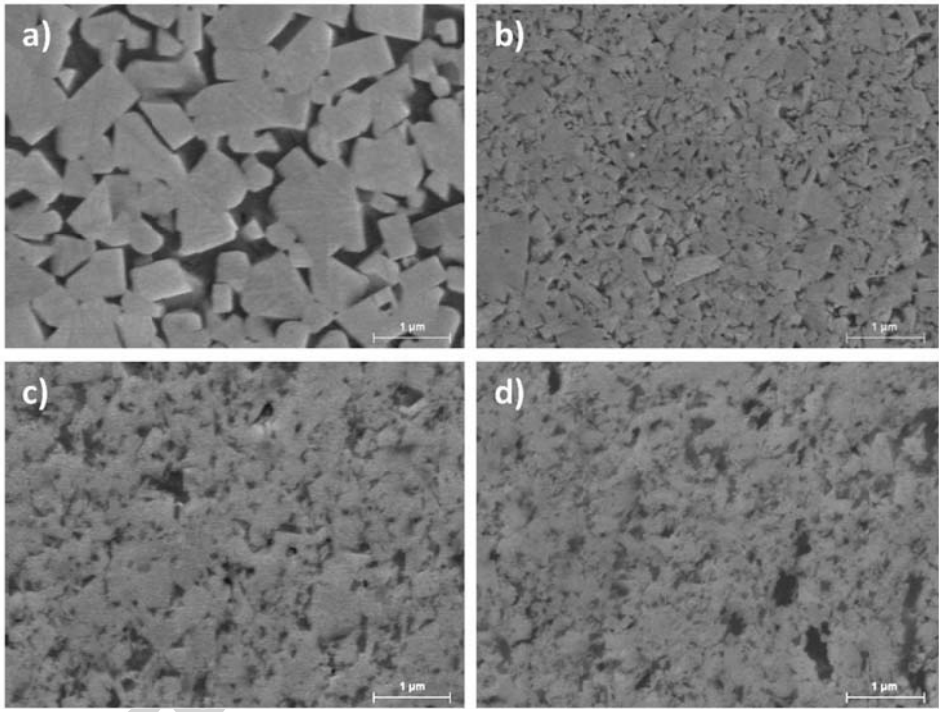

Fig. 1. FESEM micrographs of consolidated materials: a) N and b) NV, c) N-SPS and d) NV-SPS.

In both processes, there is no evidence of η- phase in any samples. Materials sintered by CS (Fig. 1a and 1b) show a microstructural control of WC grains through the VC addition (Fig. 1b), with the average grain size less than 400 nm and resulting in minimal abnormal growth. Materials consolidated by SPS (Fig. 1c and 1d) show a microstructural inhomogeneity, which is typical for the solid phase sintering with Co

segregations and lack of wettability [18]. The finest microstructure is observed in all materials sintered by SPS, even in the absence of inhibitors (Fig. 1c). The addition of inhibitors with the combination of the optimal sintering conditions in the SPS technique resulted in an effective method to obtain near-nanometric cemented carbides with an average grain size of 150 nm (Fig. 1d). The contiguity of the carbides network is greater in the SPS samples, which is caused by Co segregations that lead a high contact degree between WC grains. Samples sintered by CS shown a lower contiguity of WC grains, which indicate that there is a relatively homogeneous distribution of the Co binder phase in the WC-Co material.

Density, mean WC grain size and hardness values of consolidated materials are presented in Table 2. It should be noted that all reported data are the average of five measurements.

Table 2. Density, grain size and hardness of the materials consolidated by conventional and spark plasma sintering.

Materials	Bulk density (g/cm^3)	Relative density (%)	Mean WC grain size (μm)	Vickers Hardness HV_{30} (Kgf/mm^2)
N	14.31	99.5 ± 0.1	0.747 ± 0.038	1503 ± 15
NCr	14.09	99.1 ± 0.1	0.398 ± 0.022	1668 ± 16
NCrV	14.02	98.8 ± 0.1	0.233 ± 0.046	1822 ± 15
NV	13.98	98.7 ± 0.1	0.178 ± 0.013	1944 ± 14
N-SPS	14.37	99.9 ± 0.1	0.216 ± 0.021	1847 ± 17
NCr-SPS	14.19	99.8 ± 0.1	0.207 ± 0.011	1872 ± 17
NCrV-SPS	14.07	99.2 ± 0.1	0.190 ± 0.021	1923 ± 19

NV-SPS	13.85	98.9 ± 0.1	0.154 ± 0.014	1998 ± 24

All density values show densifications above 98% of theoretical density. It is important to note that, to achieve this high density by SPS it has only been necessary 1100 ºC and 5 min of holding time, whereas by CS 1400 ºC and 30 min of holding time conditions are required. The economic and energetic costs as well as the grain growth inhibition are significantly better by non-conventional technique.

The hardness values of the SPS sintered samples are higher than those of CS samples. The hardness increases with the reduction of WC grain size, which allow to achieve full densification. The addition of inhibitors improves the hardness in both consolidation techniques due to its effectiveness in controlling the WC grain growth during the sintering process.

3.2. Friction coefficient

The friction coefficient (μ) is the ratio between friction force and the imposed normal force. The friction force was continuously measured during the test by a load cell with a piezoelectric transducer over the loading arm. The evolution of friction coefficients has usually two different regions called non-steady or running-in state and steady state [26]. The evolution of friction coefficients for 10000 m of sliding distance of all materials tested is presented in Fig. 2.

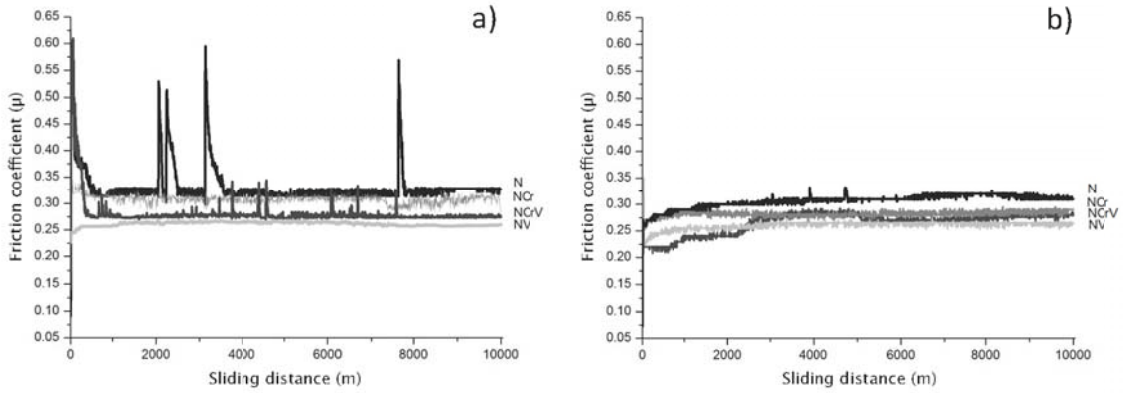

Fig. 2. Friction coefficient evolution with sliding distance for materials consolidated by: CS (a) and SPS (b).

In general, a first observation shows that the behavior of the friction coefficient is strongly influenced by inhibitor additions, especially VC, and the consolidation techniques.

The friction coefficient behavior in materials sintered by CS (Fig. 2a) can be distributed in two different groups, the first group; (N, NCr and NCrV) and, the second group; NV.

In the first group, the running-in state is extended until around 800 m of sliding distance. This behavior is determined by an abrupt removal of fragments of material, which constitute the tribopair, causing an increase in ploughing and third-body presence in the contact zone. As sliding continues, a steady state is reached and the friction coefficient decreases showing almost a constant value. This behavior can be justified with the multi-asperity contact theory exposed by Zhang et al. [27,28]. Thus, the friction coefficient values are due to three components, adhesion, asperity ploughing and debris ploughing. ~~The first one, adhesion, provides the lower contribution to friction coefficient.~~ The fluctuations observed in the friction coefficient during the test in N, NCr and NCrV materials are probably due to a low frequency

vibration that occurs in the tribometer and/or to a rupture/regeneration phenomena of the tribological layer of the wear debris.

In the second group (NV materials), the running-in state is extended to around 1200 m of the sliding distance. This stage is characterized by a small and irregular increase of the friction coefficient. This increase is related to asperity ploughing of the hard NV material on the soft counterpart [29]. The irregularities in friction coefficient can be attributed to the small contribution of the wear debris, which can act like a third-body circulating at the contact surfaces, ~~and probably is embedded in the ball surface~~. As sliding continues, a steady state is reached until the end of the test. This suggests that, an incipient formation of a wear debris layer and polishing of asperities constitute the principal causes for the friction coefficient behavior.

The friction coefficient behavior of NV materials shows an intermediate step between materials consolidated by CS and SPS. This is probably related to the influence of hardness on the friction coefficients. Therefore, materials sintered by SPS show a similar and regular friction coefficient evolution (Fig. 2b). ~~This can be attributed to the homogeneous microstructure reached using this fast-consolidation technique.~~ The running-in state is characterized by a slight increment of the friction coefficient and is extended until around 1200 m. This behavior can be attributed to a gradual break down of asperities in the countermaterial surfaces, which is more pronounced at the ball surface due to its low hardness [30]. Thus, the formation of wear debris from the ball surface is inherent. This wear debris adheres to the countermaterial (ball) forming a bed of microdebris on its surface. In this point, the friction coefficient reaches a steady state behavior. This stage is characterized by a polishing effect of

asperities and with debris adhered to the ball surface, which provides a constant friction coefficient until the end of the test.

Fig. 3 shows the average values of the friction coefficient for the evaluated materials. The standard deviation of all performed tests with the same tribopair and test conditions is less than 5% in all cases. Materials sintered by CS show higher friction coefficients in comparison with SPS materials. The generation of the WC fragments, which act like a third-body in the surface contact and the incidence of Co/Co adhesive mechanisms, contribute to the higher friction coefficient.

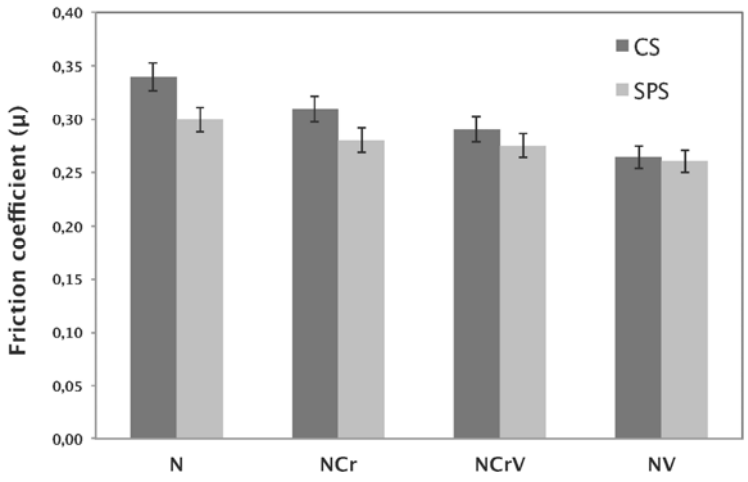

Fig. 3. Average values of friction coefficient of the sintered materials.

The friction coefficient value of the N mixture~~, sintered by CS,~~ decreases an 11.8% ~~when~~ compared to the same material (N-SPS) consolidated by the SPS technique. This behavior is due to the finest microstructure, high hardness and contiguity obtained with SPS, which minimizes the formation of wear debris and adhesion of the binder phase. In this case, the adhesive component is less likely to occur and friction

is governed by the abrasive mechanism of finer wear debris from materials on the soft counterpart (ball) surface.

On the other hand, addition of inhibitors to the mixtures allows a remarkable reduction in friction coefficients, especially VC. The friction coefficient decreases a 22% between mixture (N) and the one with 1 wt.%VC (NV). However, in the same mixtures, sintered by SPS, the reduction is 13%. Therefore, This effect is more pronounced with materials sintered by CS.

NV-SPS sample shows the lowest friction coefficient. This behavior can be explained in terms of tribological compatibility and adhesion, grain size and distribution of binder phase between WC grains [8,31-33]. Therefore, as grain size is reduced and the contiguity in WC carbides network is increased, the incidence of adhesive component of friction is reduced and the micro-abrasion mechanism over the contact surface becomes predominant [31,34].

3.3. Wear characteristics

The wear mechanism and the associated volumetric wear rate, K_v, depend critically on the precise test conditions. In general, materials tested in this study showed excellent wear resistance to dry sliding. It can be seen in Fig. 4 that the wear rates of all cemented carbides are in the order of 10^{-7} $mm^3/N{\cdot}m$.

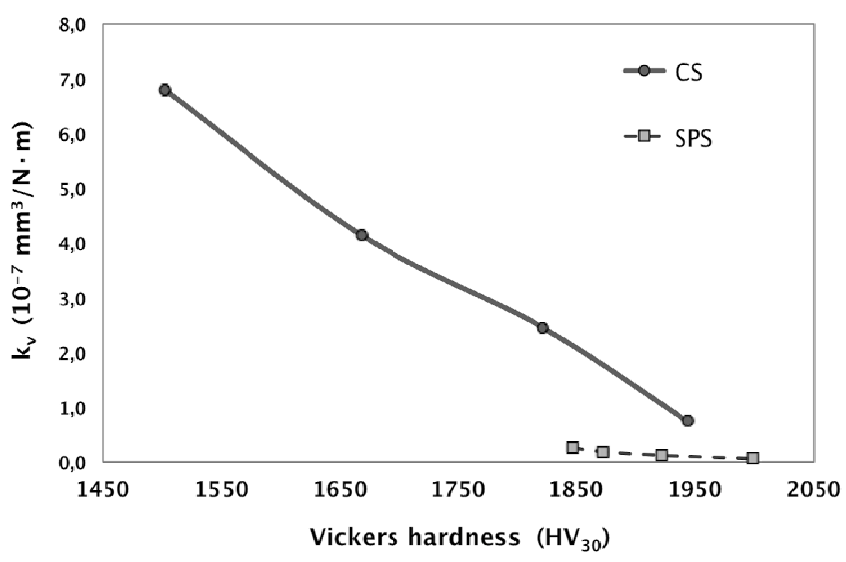

Fig. 4. Wear rate as a function of hardness for tested materials.

Materials sintered by SPS showed the best dry sliding wear resistance compared with the conventional sintered samples. Indeed, a reduction of twenty times in the wear rate was found between N and N-SPS. The wear resistance of WC-Co materials is generally considered to be a function of the WC particle size, WC content and the bonding strength of the WC particle with the cobalt matrix [2,13,16]. Hardness is usually accepted as the best indicator of wear resistance. Materials with a high hardness are usually more resistant. The optimal conditions used in the SPS technique are the principal cause of the smaller grain sizes, the improvement in hardness and a high contiguity of the WC network. Therefore, the wear resistance of materials sintered by SPS is governed for these properties, which offer resistance to pull-out of the near-nanostructured carbides.

The addition of inhibitors to mixtures, mainly VC, was found to be beneficial for the wear resistance in both sintering techniques. The improvement in the wear resistance between N-SPS and NV-SPS samples is about 75% whilst in N and NV samples is about 89%. The influence of inhibitors in samples sintered by CS is

related to the hardness increment, i.e. between N and NV is 441 HV_{30} and between N-SPS and NV-SPS is 152 HV_{30}. Consequently, the NV-SPS sample shows the lower wear rate, which is coincident with the lower friction coefficient value. It should be noted that the wear rates are obtained from the volumetric samples loss, and does not involve the wear of counterpart. In this case, the governing mechanism is polishing of asperities and microabrasion of samples surface.

3.4. Wear surface analysis

The materials consolidated by CS have a lower wear resistance in comparison with the materials consolidated by SPS. Therefore, significant differences might be expected in the wear track observations of materials consolidated by both techniques.

Wear tracks FESEM micrographs of the CS materials are presented in Fig. 5. The worn surface shows different levels of damage, which are in accordance with the obtained wear rates. The wear track analysis revealed that the wear process of the WC-Co cemented carbides obtained by CS is controlled by abrasion, grain fracture, binder removal, adhesion, grain pull-out and tribofilm formation.

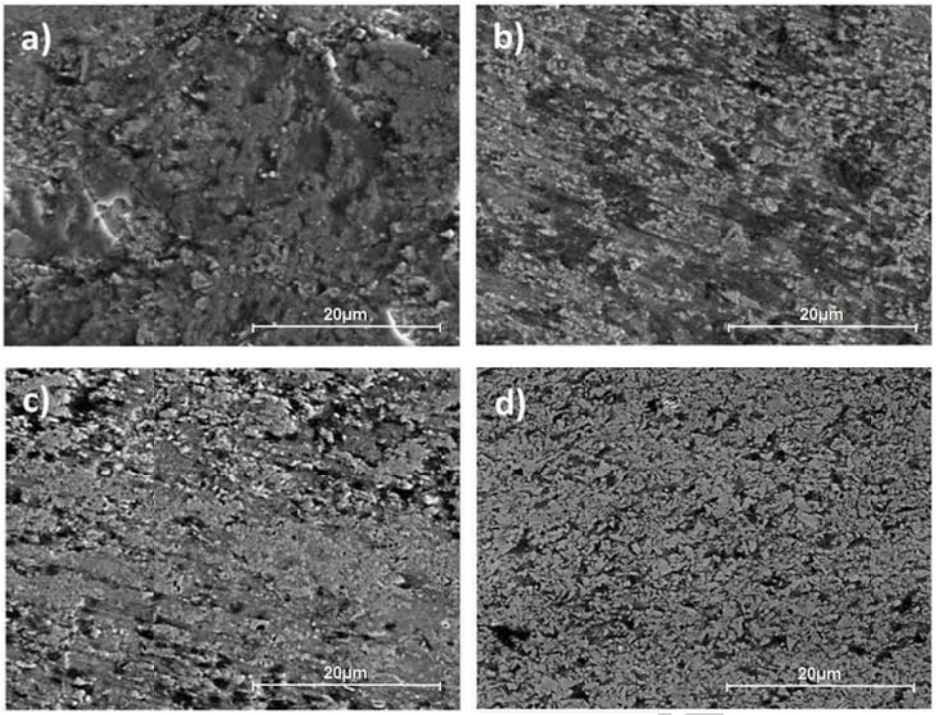

Fig. 5. FESEM micrographs of the wear tracks of the materials consolidated by CS: (a) N, (b) NCr, (c) NCrV and (d) NV.

Material without inhibitor (N) (Fig. 5a) presents the worst damage pattern due to the coexistence of several wear mechanisms. The wear track shows the appearance of a wear debris layer adhered to the surface in all areas. Some wear debris can be seen like bright spots over the surface as a consequence of the fragmentation of WC carbide grains. The Co binder phase is partially removed from the WC grain boundaries by a combination of plastic deformation and micro-abrasion, which constitutes the initial stage of wear. As sliding continues in severe test conditions, the high-pressure over the asperity contacts caused an initial WC grain micro-fragmentation. These WC micro-fragments are able to penetrate between the carbides grains and act as a third abrasive body causing an increase in removal of the cobalt binder. Moreover, the WC grains, which are not fractured, are less protected in the matrix and are more sensitive to the countermaterial pressure and

relative motion [31,35,36]. The WC phase undergoes fracture, which is attributed to the local contact load, exceeding the critical fracture limit of the WC phase [35,37]. Therefore, the wear debris products, i.e. micro-fragments of binder phase and WC grains are generated by abrasion and adhesion. The debris is entrapped and accumulates in depressions, holes and abrasion grooves on the surface and finally creates a new surface, which is gradually worn out.

The addition of inhibitors to mixtures reduces the wear damage and this is confirmed with the wear tracks observation, which follows the same behavior of Fig. 4. Thus, it is obvious that in NCr sample (Fig. 5b), the wear track presents a damage state previous to N sample. The wear tracks show grooving from abrasion in the sliding direction and carbide fragmentation, and also some holes due to Co removal. In this case, the formation of a thinner wear debris layer regarding the N sample is evident. The wear track of NCrV sample (Fig. 5c) shows the appearance of a fine and heterogeneous wear debris layer, the grooves from abrasion are slighter and the holes from Co extrusion or WC grain pull-out are fewer than the previous ones. Finally, the best wear resistance in materials sintered by CS is presented by NV sample (Fig. 5d), which is related to its high hardness values due to its smaller grain size. The wear track shows slight Co removal, WC grains micro-fragmentation, ploughing from abrasion in the sliding direction and a little submicrometre wear debris adhered to the surface.

Fig. 6a shows the wear layer of N sample, which contains a large amount of oxygen as observed in mapping of element distributions in Fig. 6b. It should be noted that the oxygen zone distribution coincides with the zones which have the most wear debris adhered. Fig. 6c shows the composition of a debris layer measured by EDX analysis

and a high oxygen concentration can be observed. The higher content of oxygen corroborates the formation of a tribolayer as a result of the elevated temperature generated in the sliding contact surface [34].

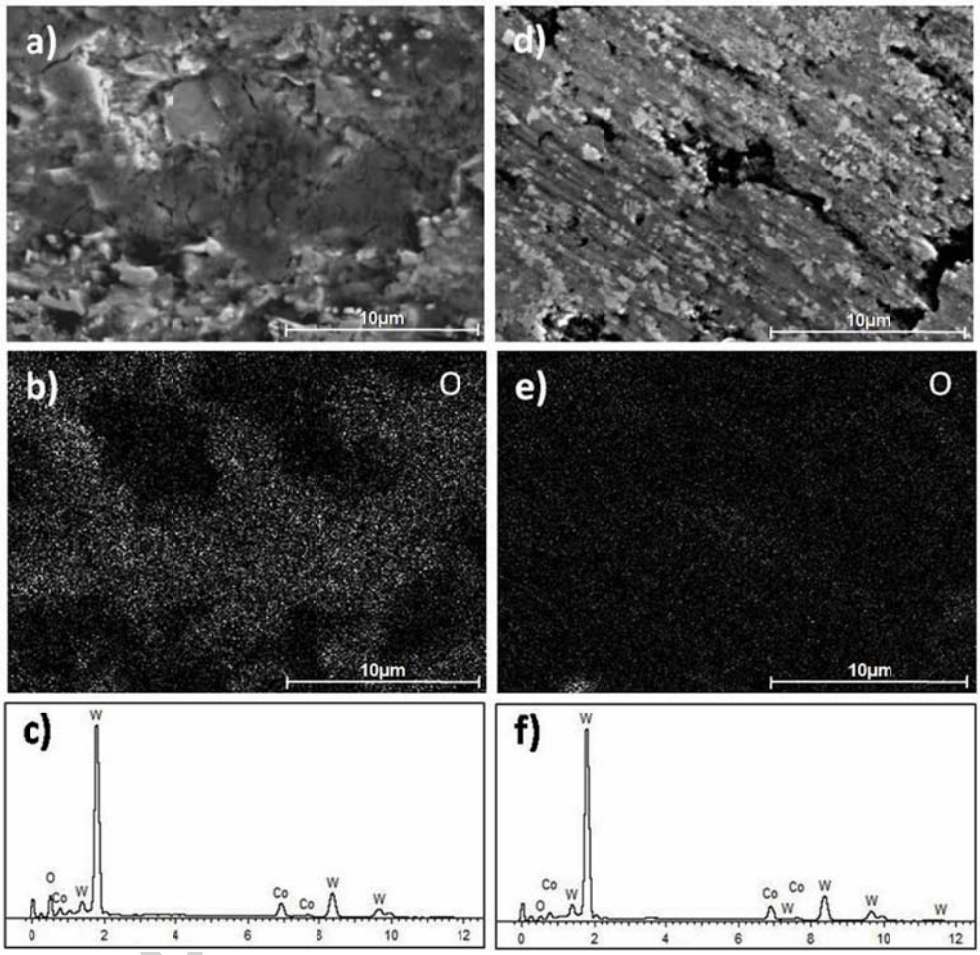

Fig. 6. FESEM micrographs of the wear tracks of N (a) and NCr (d) samples, and corresponding mapping of oxigen distribution (b, e), and EDX analysis after the test (c, f).

The mapping of oxygen distribution (Fig. 6e) and the EDX analysis (Fig. 6f) shows a reduction in the tribolayer presented in NCr material. This is due to a smaller amount of wear debris generated and because of the lower temperature reached in the sliding contact surface, which is related to the decrease of friction coefficient value.

As expected, in materials with VC addition (NCrV and NV samples), which have higher hardness values and smaller grain sizes, the wear rate is lower compared with the previous ones.

FESEM micrographs of the center track of N-SPS and NCr-SPS materials (Fig. 7a and 7c) show that the wear damage of SPS materials is reduced with respect to materials sintered by CS.

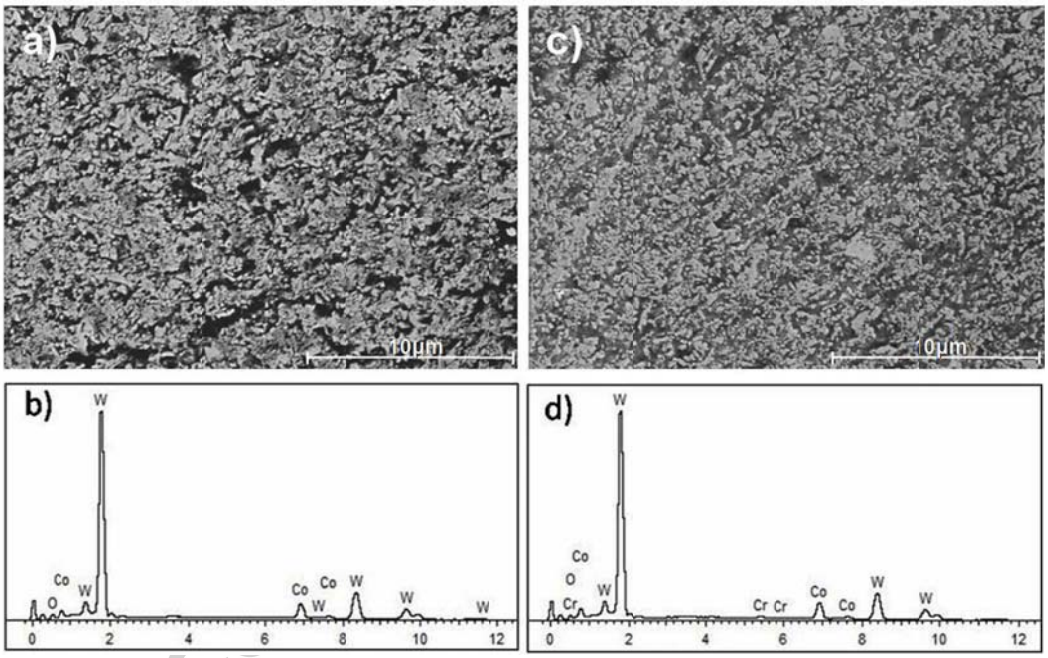

Fig. 7. FESEM micrographs of the wear tracks of N-SPS (a) and NCr-SPS (c) samples, and EDX analysis after the test (b, d).

The wear mechanism is similar in all materials sintered by SPS. However, some reduction in wear track damage is observed between them, which follows the same behavior of wear rates found. The level of wear shows the same order of magnitude as that one found in the NV material, which are in good agreement with wear rate evolution. Therefore, the wear process is mainly controlled by ploughing for abrasion

in the sliding movement, the Co binder phase extrusion and WC micro-fragmentation [36,38]. Moreover, a little wear debris due to WC micro-fragmentation remains over the surface or still inside the holes due to WC grain pull-out. A tribolayer of wear debris is clearly being created by this process. The addition of grain size inhibitors to mixtures reduces the wear damage as can be seen in Fig. 7c. The EDX analysis (Fig. 7d) shows absence of oxygen, which is in agreement with the low probability of a tribolayer formation.

In addition, the magnified FESEM micrograph of the N-SPS wear track (Fig. 8) shows the WC grain fracture (complete circles), the discontinuous circle is Co binder phase removed, and low wear debris revealed as bright spots accumulated in the holes formed by material pull-out (square).

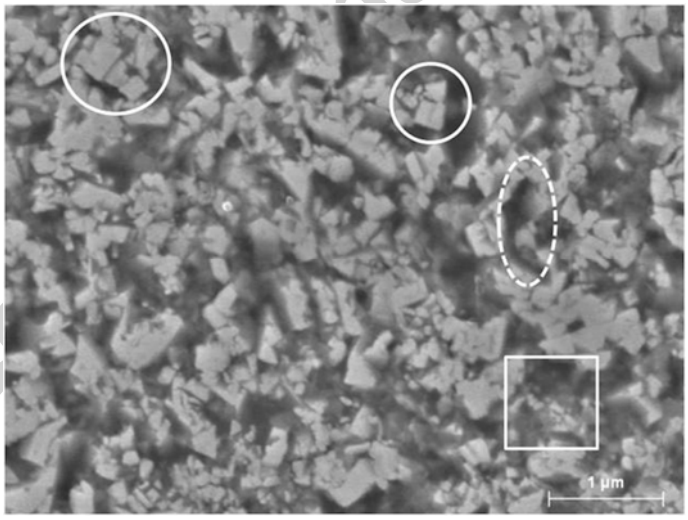

Fig. 8. FESEM detail of the N-SPS sample.

4. Conclusions

The friction and wear behavior of cemented carbides WC-Co with and without addition of grain growth inhibitors and fabricated by two sintering techniques, were evaluated using a ball-on-disk tribometer. The following conclusions were obtained:

1. It has been found that there is a relevant reduction in friction coefficient when materials are sintered by SPS technique. The addition of inhibitors makes a notable contribution to the reduction of this parameter.

2. It has been seen that there is a remarkable reduction in the wear rate when materials are sintered by SPS. The wear rate values are about twenty times lower in a mixture consolidated by SPS respect to materials sintering by CS.

3. The good sliding wear resistance in SPS consolidated materials were attributed to the fine microstructure of the material. It has been proven that the presence of inhibitors improves the wear resistance in both consolidation techniques, especially with VC. However, this effect is more noticeable in materials sintered by CS, which was attributed to the important increase in hardness.

4. The wear process in SPS materials is mainly controlled by ploughing for abrasion in the sliding movement, the Co binder phase extrusion and WC micro-fragmentation. Materials sintered by CS show the worst damage patterns and the coexistence of several wear mechanisms.

Acknowledgement

The work is supported financially by the Spanish Ministry of Science and Innovation by the project MAT2009-14144-C03-C02. L. Espinosa-Fernández, acknowledges the

AECI program for the realization of the Ph.D in the ITM-UPV. A. Borrell, acknowledges the Spanish Ministry of Science and Innovation for her *Juan de la Cierva* contract (JCI-2011-10498).

References

[1] H.O. Andren, Microstructure development during sintering and heat-treatment of cemented carbides and cermets, Materials Chemistry and Physics, 67 (2001) 209-213.

[2] R.B. Bhagat, J.C. Conway, M.F. Amateau, R.A. Brezler, Tribological performance evaluation of tungsten carbide-based cermets and development of a fracture mechanics wear model, Wear 996 (2011) 233-243.

[3] U. Beste, E. Coronel, S. Jacobson, Wear induced material modifications of cemented carbide rock drill buttons, International Journal of Refractory Metals and Hard Materials, 24 (2006) 168-176.

[4] C. Jia, L. Sun, H. Tang, X. Qu, Hot pressing of nanometer WC-Co powder, International Journal of Refractory Metals and Hard Materials, 25 (2007) 53-56.

[5] G. Gille, B. Szesny, K. Dreyer, H. Van Den Berg, J. Schmidt, T. Gestrich, G. Leitner, Submicron and ultrafine grained hardmetals for microdrills and metal cutting inserts, International Journal of Refractory Metals and Hard Materials, 20 (2002) 3-22.

[6] C.C. Jia, H. Tang, X.Z. Mei, F.Z. Yin, X.H. Qu, Spark plasma sintering on nanometer scale WC-Co powder, Materials Letter, 59 (2005) 2566-2569.

[7] S. Zhao, X. Song, C. Wei, L. Zhang, X. Liu, J. Zhang, Effects of WC particle size on densification and properties of spark plasma sintered WC-Co cermet, International Journal of Refractory Metals and Hard Materials, 27 (2009)

1014-1018.

[8] K. Jia, T.E. Fischer, Sliding wear of conventional and nanostructured cemented carbides, Wear 203-204 (1997) 310-318.

[9] D.F. Carroll, Sintering and microstructural development in WC/Co-based alloys made with superfine WC powder, International Journal of Refractory Metals and Hard Materials, 17 (1999) 123-132.

[10] Z.Z. Fang, J.W. Eason, Study of nanostructured WC-Co composites, International Journal of Refractory Metals and Hard Materials, 13 (1995) 297-303.

[11] I. Azcona, A. Ordoñez, J.M. Sánchez, F. Castro, Hot isostatic pressing of ultrafine tungsten carbide-cobalt hard metals, Journal of Materials Science, 37 (2002) 4189-4195.

[12] E. Breval, J.P. Cheng, D.K. Agrawal, P. Gigl, M. Dennis, R. Roy, AJ. Papworth, Comparison between microwave and conventional sintering of WC/Co composites, Materials Science and Engineering: A 391 (2005) 285-295.

[13] J. Zhao, T. Holland, C. Unuvar, ZA. Munir, Spark plasma sintering of nanometric tungsten carbide, International Journal of Refractory Metals and Hard Materials, 27 (2009) 130-139.

[14] S.G. Huang, K. Vanmenensel, L. Li, O. Van Der Biest, J. Vleugels, Influence of starting powder on the microstructure of WC-Co hardmetals obtained by spark plasma sintering, Materials Science and Engineering: A 475 (2008) 87-91.

[15] D. Sivaprahasam, S.B. Chandrasekar, R. Sundaresan, Microstructure and mechanical properties of nanocrystalline WC-12Co consolidated by spark plasma sintering, International Journal of Refractory Metals and Hard

Materials, 25 (2007) 144-152.

[16] J.A. Picas, Y. Xiong, M. Punset, L. Ajdelsztajn, A. Forn, J.M. Schoenung, Microstructure and wear resistance of WC-Co by three consolidation processing techniques, International Journal of Refractory Metals and Hard Materials, 27 (2009) 344-349.

[17] X. Sun, Y. Wang, D.Y. Li, Mechanical properties and erosion resistance of ceria nano-particle-doped ultrafine WC-12Co composite prepared by spark plasma sintering, Wear 301 (1-2) (2013) 406-414.

[18] V. Bonache, M.D. Salvador, A. Fernández, A. Borrell, Fabrication of full density near-nanostructured cemented carbides by combination of VC/Cr_3C_2 addition and consolidation by SPS and HIP technologies, International Journal of Refractory Metals and Hard Materials, 29 (2011) 202-208.

[19] A.G.P. Da Silva, C.P. De Souza, U.U. Gomes, F.F.P. Medeiros, C. Ciaravino, M. Roubin, A low temperature synthesized NbC as grain growth inhibitor for WC-Co composites, Materials Science and Engineering: A 293 (2000) 242-246.

[20] V. Bonache, M.D. Salvador, D. Busquets, E.F. Segovia, Fabrication of ultrafine and nanocrystalline WC-Co mixtures by planetary milling and subsequent consolidations, Powder metallurgy 54 (2011) 214-221.

[21] ISO 3369: 2006. Impermeable sintered metal materials and hardmetals-Determination of density.

[22] ASTM E112-96. Standard test methods for determining average grain size. 2004.

[23] ISO 3078-1983: Hardmetals. Vickers hardness test.

[24] ASTM G99-03. Standard test method for wear testing with a pin-on-disc apparatus, ASTM Annual Book of Standards, Vol. 03.02, West

Conshohocken, PA, 2003.

[25] J.K. Lancaster, The influence of substrate hardness on the formation and endurance of molybdenum disulphide films, Wear 10 (1966) 103-117.

[26] V. Fervel, B. Normand, C. Coddet, Tribological behavior of plasma sprayed Al_2O_3-based cermet coatings, Wear 230 (1999) 70-77.

[27] J. Zhang, F.A. Moslehy, S.L. Rice, A model for friction in quasi-steady-state. Part I. Derivation, Wear 149 (1991) 1-12.

[28] J. Zhang, F.A. Moslehy, S.L. Rice, A model for friction in quasi-steady-state sliding Part II. Numerical results and discussion, Wear 149 (1991) 13-25.

[29] Q. Luo, Origin of friction in running-in sliding wear of nitride coatings, Tribology Letters, 37 (2010) 529-539.

[30] S. Achanta, J.P. Celis, On the scale dependence of coefficient of friction in unlubricated sliding contacts, Wear 269 (2010) 435-442.

[31] K. Bonny, P. De Baets, J. Vleugels, S. Huang, O. Van Der Biest, B. Lauwers, Impact of Cr_3C_2/VC addition on the dry sliding friction and wear response of WC-Co cemented carbides, Wear 267 (2009) 1642-1652.

[32] J.Y. Sheikh-Ahmad, J.A. Bailey, The wear characteristics of some cemented tungsten carbides in machining particleboard, Wear 225-229 (1999) 256-266.

[33] J. Pirso, M. Viljus, S. Letunovits, Friction and dry sliding wear behaviour of cermets, Wear 260 (2006) 815-824.

[34] H. Engqvist, G.A. Botton, S. Ederyd, M. Phaneuf, J. Fondelius, N. Axen, Wear phenomena on WC-based face seal rings, International Journal of Refractory Metals and Hard Materials, 18 (2000) 39-46.

[35] K. Bonny, P. de Baets, J. Vleugels, B. Lauwers, Dry reciprocating sliding friction and wear response of WC-Ni cemented carbides, Tribology Letters, 31 (2008) 199-209.

[36] J. Larsen-Basse, Binder extrusion in sliding wear of WC-Co alloys, Wear 105 (1985) 247-256.

[37] L. Espinosa, V. Bonache, M.D. Salvador, Friction and wear behaviour of WC-Co-Cr_3C_2-VC cemented carbides obtained from nanocrystalline mixtures, Wear 272 (2011) 62-68.

[38] D. Jianxin, Z. Hui, W. Ze, L. Yunsong, Z. Jun, Friction and wear behaviors of WC/Co cemented carbide tool materials with different WC grain sizes at temperatures up to 600ºC, International Journal of Refractory Metals and Hard Materials, 31 (2012) 196-204.

Highlights

- An important reduction is observed on the friction coefficient in SPS materials.
- The inhibitors have more influence in the friction coefficient of CS materials.
- The SPS technique provides materials with an excellent sliding wear resistance.
- The wear rates are about twenty times lower in SPS mixtures respect to CS materials.
- The increments in dry sliding wear resistance with inhibitors have been proven.